Inflammation Research
https://doi.org/10.1007/s00011-024-01941-1

Inflammation Research

ORIGINAL RESEARCH PAPER

Simultaneously blocking ANGPTL3 and IL-1β for the treatment of atherosclerosis through lipid-lowering and anti-inflammation

Hanqi Wang[1,2] · Xiaozhi Hu[2] · Yuting Zhang[2] · An Zhu[2] · Jiajun Fan[2] · Zhengyu Wu[3] · Xuebin Wang[4] · Wei Hu[1] · Dianwen Ju[1,2]

Received: 4 July 2024 / Revised: 10 August 2024 / Accepted: 29 August 2024

Abstract

Objective Blood lipid levels play a critical role in the progression of atherosclerosis. However, even with adequate lipid reduction, significant residual cardiovascular risk remains. Therefore, it is necessary to seek novel therapeutic strategies for atherosclerosis that can not only lower lipid levels but also inhibit inflammation simultaneously.

Methods The fusion protein FD03-IL-1Ra was designed by linking the Angiopoietin-like 3 (ANGPTL3) nanobody and human interleukin-1 receptor antagonist (IL-1Ra) sequences to a mutated human immunoglobulin gamma 1 (IgG1) Fc. This construct was transfected into HEK293 cells for expression. The purity and thermal stability of the fusion protein were assessed using SDS-PAGE, SEC-HPLC, and differential scanning calorimetry. Binding affinities of the fusion protein to ANGPTL3 and IL-1 receptor were measured using Biacore T200. The biological activity of the fusion protein was validated through in vitro experiments. The therapeutic efficacy of the fusion protein was evaluated in an ApoE-/- mouse model of atherosclerosis, including serum lipid level determination, histological analysis of aorta and aortic sinus sections, and detection of inflammatory and oxidative stress markers. ImageJ software was utilized for quantitative image analysis. Statistical analysis was performed using one-way ANOVA followed by Bonferroni post hoc test.

Results The FD03-IL-1Ra fusion protein was successfully expressed, with no polymer formation detected, and it demonstrated good thermal and conformational stability. High affinity for both murine and human ANGPTL3 was exhibited by FD03-IL-1Ra, and it was able to antagonize hANGPTL3's inhibition of LPL activity. FD03-IL-1Ra also showed high affinity for both murine and human IL-1R, inhibiting IL-6 expression in A549 cells induced by IL-1β stimulation, as well as suppressing IL-1β-induced activity inhibition in A375.S2 cells. Our study revealed that the fusion protein effectively lowered serum lipid levels and alleviated inflammatory responses in mice. Furthermore, the fusion protein enhanced plaque stability by increasing collagen content within atherosclerotic plaques.

Conclusions These findings highlighted the potential of bifunctional interleukin-1 receptor antagonist and ANGPTL3 antibody fusion proteins for ameliorating the progression of atherosclerosis, presenting a promising novel therapeutic approach targeting both inflammation and lipid levels.

Keywords Atherosclerosis · ANGPTL3 · IL-1Ra · Fusion protein

Introduction

Atherosclerosis serves as the primary pathological foundation for ischemic cardiovascular diseases (CVD), and the projected mortality due to CVD in 2030 is estimated to reach 22.2 million [1]. This condition is influenced by various pathogenic factors, including elevated blood lipid levels, inflammation, and oxidative stress [2]. Current clinical approaches to atherosclerosis primarily involve medications such as statins and proprotein convertase subtilisin/kexin type 9 (PCSK9) inhibitors [3]. However, despite achieving sufficient reductions in serum lipid levels, a substantial residual cardiovascular risk persists [3, 4]. Consequently, exploring innovative avenues for preventing and treating atherosclerosis.

Responsible Editor: John Di Battista.

Hanqi Wang, Xiaozhi Hu, Yuting Zhang have contributed equally to this work.

Extended author information available on the last page of the article

Published online: 10 September 2024

Elevated blood lipid levels have been identified as a critical contributor to atherosclerosis. Notably, a reduction of 1 mmol/L in low-density lipoprotein cholesterol (LDL-C) is associated with a 23% risk decrease for CVD [5]. However, despite statin monotherapy achieving a 50% reduction in LDL-C levels at maximum dosages, over half of the patients show minimal response, highlighting the necessity of an alternative approach [6, 7]. Angiopoietin-like protein 3 (ANGPTL3), a member of the angiopoietin-like protein family, participates in lipid metabolism, inhibits lipoprotein lipase (LPL) activity, and contributes to angiogenesis in vivo [8, 9]. Increased levels of ANGPTL3 are positively correlated with an elevated risk of CVD. Conversely, the loss of ANGPTL3 function reduces the risk by approximately 34% in individuals with normal lipid profiles [10]. Neutralizing ANGPTL3 with evinacumab demonstrated efficacy in reducing plasma levels of total cholesterol (TC), triglyceride (TG), and LDL-C, even in individuals with homozygous familial hypercholesterolemia who are unresponsive to conventional lipid-lowering therapies targeting LDL receptor (LDLR) and PCSK9 mutations [11]. In our initial investigations, the administration of a nanobody-Fc (FD03) directed against ANGPTL3 led to a substantial reduction in TG, TC, and LDL-C in hypercholesterolemic mice. Notably, a higher expression yield was observed compared to evinacumab [12]. Accordingly, we propose that FD03 can be a promising therapeutic agent for atherosclerosis through lipid-lowering interventions.

Recent evidence has compellingly highlighted the crucial role of inflammation in driving atherosclerosis's pathogenesis. Interleukin-1β (IL-1β) is a key inflammatory factor that regulates the innate immune response in blood vessels and influences cytokine secretion [13]. Abundant research has underscored the significant impact of IL-1β on atherosclerosis [14, 15]. Noteworthy, elevated levels of IL-1β expression were found to positively correlate with the risk of acute cardiovascular events due to plaque rupture, which has been observed in individuals with atherosclerosis [16–18]. In atherosclerotic mice, the knockdown of IL-1β has been shown to substantially reduce atherosclerotic lesions and improve plaque stabilization. This effect is attributed to the decreased levels of inflammatory cytokines, including IL-6 and TNF-α [19–23]. Anakinra is a recombinant IL-1Ra consisting of 153 amino acid residues but with an additional methionine residue at the amino terminus. It has been shown to effectively reduce IL-1β and C-reactive protein levels in patients' serum, offering relief from heart failure associated with atherosclerotic complications [24, 25]. Oxidative stress can influence the progression of atherosclerosis by modulating endothelial vascular function, regulating vascular smooth muscle cell growth, and affecting macrophage immune and inflammatory responses [26]. 4-Hydroxynonenal (4-HNE) is a reactive aldehyde formed by the reaction of reactive oxygen species with polyunsaturated fatty acids, and it is often associated with cellular dysfunction and tissue damage, thereby exacerbating atherosclerosis [27]. Therefore, we hypothesize that simultaneously inhibiting ANGPTL3 and IL-1β to regulate lipid metabolism and inflammation can reduce oxidative stress levels and lead to better outcomes in the treatment of atherosclerosis.

In this study, a novel fusion protein, FD03-IL-1Ra, was successfully generated by linking human IL-1Ra to the C-terminus of FD03. Subsequently, its stability and biological activity in blocking ANGPTL3 and IL-1β were assessed. Furthermore, the beneficial effects of FD03-IL-1Ra on atherosclerosis were validated, highlighting its dual efficacy in reducing lipid deposition and concurrently suppressing the inflammatory response. The potential of the FD03-IL-1Ra fusion protein as a promising therapeutic approach for addressing atherosclerosis was emphasized by these results.

Materials and methods

Preparation of FD03, IL-1Ra-Fc and FD03-IL-1Ra fusion protein

The gene encoding FD03 was obtained from research conducted by Dr. Dianwen Ju's lab, linking the sequence of the anti-ANTPTL3 nanobody to the human immunoglobulin gamma 1 (IgG1) Fc through a flexible linker, incorporating the hinge region with mutating of 82 Asn/Ala, 141 Asp/Glu and 143 Leu/Met. The genes encoding these fusion proteins, along with FD03, were inserted into PPT5 plasmid vectors. The aforementioned plasmids were employed in the HEK293 expression system for expression and purification, leading to the isolation of the target proteins.

Plasmids were transferred to chemically competent cells, amplified in LB medium, and extracted using EndoFree Maxi plasmid large kits (Tiangen, Beijing, China). All three expression plasmids were introduced into Expi293F cells using PEI MAX (Yesen, Shanghai, China), and the cell supernatants were harvested 8 days post-transfection. Subsequently, all supernatants were purified using rProtein A Seplife Suno column (Sunresin, Suzhou, China) on an AKTA purifier (Cytiva, MA, United States).

Cell culture

Expi293F and A549 cell lines were sourced from the National Collection of Authenticated Cell Cultures (Shanghai, China), while A375.S2 cells were graciously provided by Professor Shuqing Chen of Zhejiang University. Expi293F cells underwent cultivation in SMM 293-TII complete medium (Sino Biological Inc., Beijing, China) with agitation at 120 RPM and 50 mm amplitude on a cell

shaker (Thermo Fisher Scientific). A549 and A375.S2 cells were nurtured in RPMI base medium (Yuanpei, Shanghai, China) supplemented with FBS (Gibco, 10,270). Incubation occurred at 37 ℃ within a humidified atmosphere featuring 5% CO_2 in an incubator.

SDS-PAGE analysis

SDS-PAGE analysis under both reduced and non-reduced conditions was conducted using the PAGE Gel Fast Preparation Kit (10%, Yamei, Shanghai, China) and Tris–Glycine SDS running buffer. Each protein sample, with a loading amount of 10 μg, was electrophoresed at 120 V for 40 min. Gels were stained with Meilunbio ultrafast gel protein staining solution (MeilunBio, Dalian, China) and destained in ultra-pure grade water.

Monomeric purity determination

The monomeric purity of the fusion protein was assessed employing the Agilent 1260 system. A mobile phase of PBS and protein samples (120 μg) were passed through a TOSOH TSKgel G3000WXL column at 1 ml/min, with UV absorbance at 280 nm OD value for 30 min.

Differential scanning calorimetry (DSC)

MicroCal VP-DSC (Microcal LLC) was utilized to measure the differential scanning calorimetry (DSC) of the three fusion proteins. The data were fitted to MN2State model by Origin 3.0 SR2.

Affinity determination of fusion proteins

The Biacore T200 was employed for measuring the affinity of FD03 and FD03-IL-1Ra binding to human full-length ANGPTL3 (hANGPTL3 (S17-E460)-His10), murine half-length ANGPTL3 (mANGPTL3 (S17-T206)-His6), and murine full-length ANGPTL3 (mANGPTL3 (S17-T455)-His10), as well as IL-1Ra-Fc and FD03-IL-1Ra binding to hIL-1R1 (18–332)-His6 and mIL-1R1 (20–338)-His6 using surface plasmon resonance (SPR). ANGPTL3 and IL-1R were immobilized on the CM5 chip (Cytiva, MA, United States), and the fusion proteins, diluted in EP buffer, were passed through the chip at 150 s and permitted to dissociate for 480 s. The affinity (KD) was determined by the Biacore Evaluation software.

Anti-angptl3 biological activity test in vitro

Fusion proteins, evinacumab and a control antibody, were incubated with hANGPTL3 (S17-K170)-mFc. This complex was then incubated with 50 nM bovine LPL (Yingxin, Shanghai, China) in an assay buffer comprising 20 mM Tris, 150 mM NaCl and 0.2% fatty-acid-free BSA at pH 8.0.

After incubation with 10 μM Lipase Substrate (30,058, Sigma) for 15 min at 25 °C in black-walled 96-well plates (Corning Glass), fluorescence was measured on a microplate reader using an excitation wavelength of 529 nm and reading emission at 600 nm.

Determination of IL-1β antagonism in vitro

A549 cells (1×10^4 cells/well) were plated in 96-well plates (Corning Glass) and treated with varying concentrations of FD03-IL-1Ra, IL-1Ra-Fc, IL-1Ra (Jiaochen, Shanghai, China), and FD03 for 1 h after cell attachment. Subsequently, cells were stimulated with 200 pg/ml recombinant human IL-1β (Abclonal, Wuhan, China) for 6 h. The culture medium from stimulated A549 cells was collected and subjected to IL-6 level analysis utilizing a human IL-6 ELISA kit (Abclonal, Wuhan, China).

A375.S2 cells were digested, centrifuged, and resuspended in RPMI 1640 medium (2% FBS). After 12 h, gradient concentrations of FD03-IL-1Ra, IL-1Ra-Fc, IL-1Ra, and FD03 were added to the culture medium. An hour later, IL-1β was added at a concentration of 20 ng/ml and incubated for 72 h. Cell growth inhibition was determined using a microplate reader (Thermo) after the addition of 10% Meilun Cell Counting Kit-8 (Meilun, Dalian, China) solution, with absorbance measured at 450 nm.

Animals

$ApoE^{-/-}$ mice (male, 6–8 weeks old) were procured from Cavins Animal. Atherosclerotic plaque induction was achieved by feeding the mice a high-fat diet (HFD) constituting 20% fat, 1.25% cholesterol, and 0.2% bile salt for 14 weeks [22].

After 8 weeks of dietary treatment, mice were randomly allocated into six groups for comparative drug effect assessment on atherosclerosis: Control ab-treated group (n = 6, 25 mg/kg, intraperitoneal injection once weekly for 5 weeks), FD03-treated group (n = 6, 25 mg/kg, intraperitoneal injection once weekly for 5 weeks), IL-1Ra-Fc-treated group (n = 6, 28.7 mg/kg, intraperitoneal injection once weekly for 5 weeks), Combinational drugs-treated group (n = 6, 25 mg/kg and 28.7 mg/kg, intraperitoneal injection once weekly for 5 weeks), FD03-IL-1Ra-treated group (n = 6, 37.6 mg/kg, intraperitoneal injection once weekly for 5 weeks) and Positive drug Atorvastatin-treated group (n = 6, 10 mg/kg, intragastric administration once daily for 5 weeks).

FD03 group, IL-1Ra-Fc group, and FD03-IL-1Ra group received equimolar administration (molecular weight: FD03 ~ 76.9 kD; IL-1Ra-Fc ~ 88.2 kD, FD03-IL-1Ra ~ 115.8

kD). Serum samples were collected from the mouse orbit 4 days after each injection and storage at -80 °C.

Metabolism and cytokine assays

Blood samples were collected from the mouse orbit following four days of weekly dosing. Serum triglyceride, total cholesterol, and LDL-C levels were quantified using an assay kit from NanJingJianCheng, Nanjing, China. Additionally, serum samples collected at week 5 underwent analysis for IL-1β, IL-6, and TNF-α utilizing ELISA kits. All assays were conducted in strict adherence to the instructions provided with the respective kits.

Morphological and atherosclerotic lesion area staining of the aorta

After euthanasia, the mice underwent dissection, and perfusion with PBS from the left ventricle was performed until the liver achieved a white appearance. The surrounding adventitial fatty tissue was meticulously dissected. Intact aortas were then extracted, and any residual blood and fat were further eliminated in PBS. The aortas were subsequently fixed in 10% paraformaldehyde for one hour. The aorta was longitudinally dissected with a spring scissor and immersed in 60% Oil Red O dye solution, followed by incubation in a 37 ℃ water bath for 30 min. After discarding the Oil Red stain, differentiation was carried out twice using 75% ethanol for 5 min each. Ethanol was then washed off with PBS. Photographs of the aortas were taken, and the entire intima and plaque area were quantified using ImageJ software (NIH, Bethesda, MA, USA). The ratio of intima area occupied by plaques was calculated as part of the analysis.

Histopathological study of aortic sinus

After sacrificing the mice, the hearts were fixed in 10% paraformaldehyde (Servicebio). Subsequently, they were embedded in OCT, and 4-μm-thick slices were prepared. To assess the morphology, stability, and lipid content of atherosclerotic plaques, frozen sections of the aortic sinus underwent staining with hematoxylin and eosin (H&E), masson trichrome (Masson), and Oil Red O. The stained sections were then observed using a section scanner (VS200, Olympus, USA).

For quantification, the scanned aortic sections were converted to grayscale images and the scale was set. The analysis region was delineated along the inner wall of the vessel, and the threshold was adjusted to highlight the positive areas. The positive area was then measured using Fiji software. This analysis aimed to provide insights into the characteristics of atherosclerotic plaques in the examined heart tissues.

Immunohistochemical and immunofluorescence analysis of aortic sinus

The frozen sections were brought to room temperature, incubated in 0.1% Triton X-100 for ten minutes, and then blocked for nonspecific binding with 5% BSA. For immunohistochemical (IHC) staining of DCFH-DA (1:500), with Hoechst labeling of the nuclei, the aim was to investigate the impact of fusion proteins on the liberation of reactive oxygen species. Additionally, immunofluorescence analysis of 4-HNE (Abcam, 1:100) was conducted to measure the effect of fusion proteins in inhibiting oxidative stress. ImageJ software was employed for the calculation of all results.

Statistical analysis

All data were presented as means ± standard error of the mean (SEM). Multiple group comparisons were conducted using one-way ANOVA followed by Bonferroni post hoc test. A P-value less than 0.05 ($P < 0.05$) was considered significant. Statistically significant differences were denoted as $^{*}P < 0.05$, $^{**}P < 0.01$, or $^{***}P < 0.001$.

Results

Preparation of FD03-IL-1Ra fusion protein

To develop the anti-ANGPTL3/IL-1Ra fusion protein (FD03-IL-1Ra), the N-terminus of the mutated human IgG1 Fc domain was attached to the anti-ANGPTL3 FD03 nanobody, while the C-terminus of IgG1 Fc was connected to human-derived IL-1Ra through a flexible linker (Gly4Ser triplicate) (Fig. 1A). The molecular weight of the fusion proteins was determined by SDS-PAGE (Fig. 1B). The purity of FD03-IL-1Ra was confirmed by the size-exclusion chromatography (sec-HPLC), no polymers were founded (Fig. 1C). The Tm1 values of FD03-IL-1Ra, IL-1Ra-Fc, and FD03 fusion proteins were determined as 56.73 ℃, 55.95 ℃, and 58.29 ℃, respectively (Fig. 1D, E). All main peaks maintained a purity of over 95% after multiple freeze–thaw cycles (Fig. 1F), indicating robust stability of the fusion proteins.

Binding affinity and biological activity of FD03-IL-1Ra fusion proteins against ANGPTL3

The binding affinity of FD03-IL-1Ra and FD03 to ANGPTL3 was assessed by surface plasmon resonance (SPR). FD03-IL-1Ra demonstrated outstanding affinity to murine full-length ANGPTL3 at 0.4967 nM, human full-length ANGPTL3 at 0.555 nM, and murine half-length

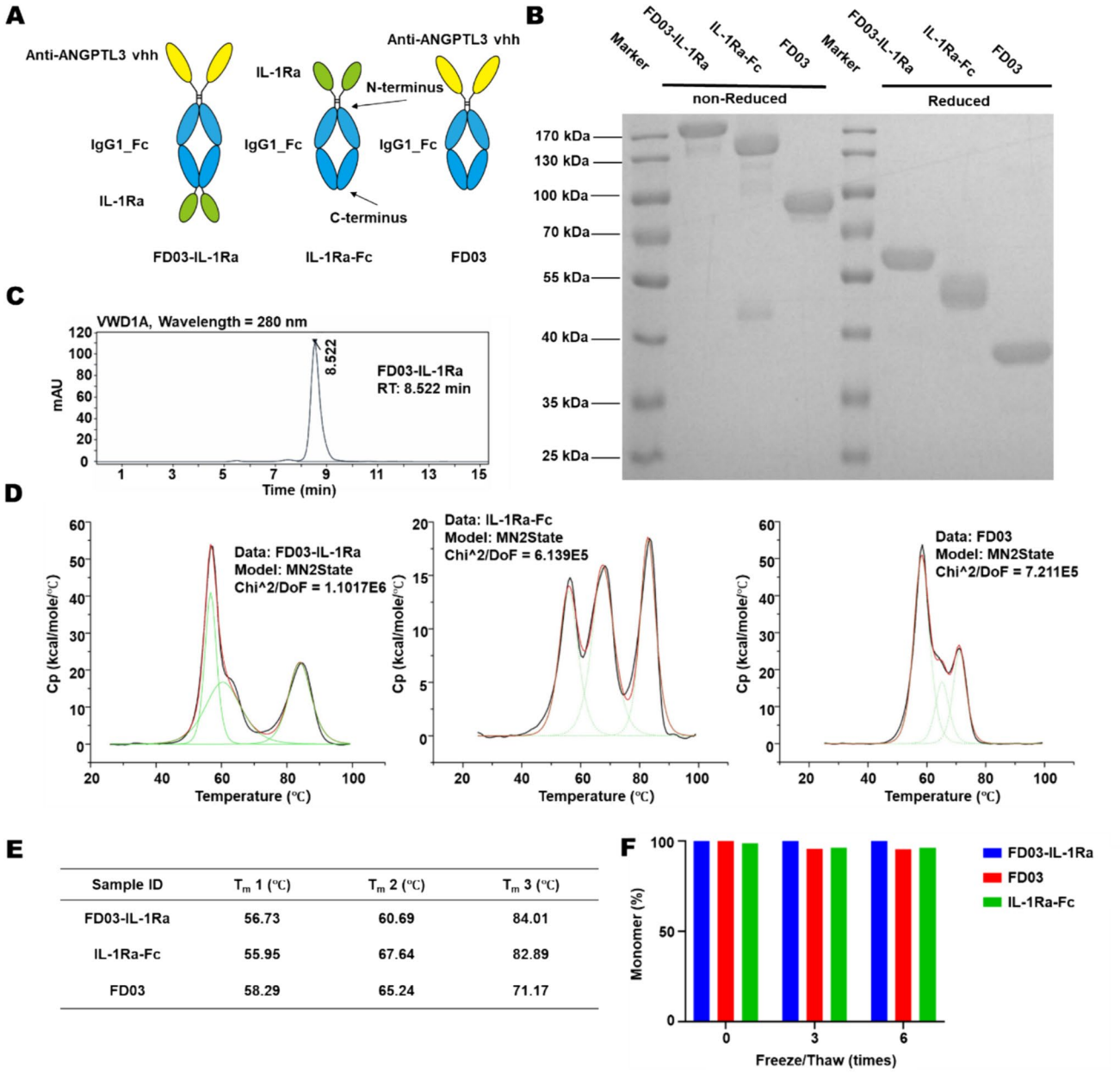

Sample ID	T_m 1 (℃)	T_m 2 (℃)	T_m 3 (℃)
FD03-IL-1Ra	56.73	60.69	84.01
IL-1Ra-Fc	55.95	67.64	82.89
FD03	58.29	65.24	71.17

Fig. 1 Preparation of FD03-IL-1Ra fusion protein. **A** Diagram of the FD03-IL-1Ra, IL-1Ra-Fc and FD03. **B** Relative SDS-PAGE analysis of fusion proteins expressed using HEK293 cells. A 10% gel was used, and electrophoresis was performed at 120 V for 40 min. **C** SEC-HPLC profile of purified FD03-IL-1Ra fusion protein. **D** Thermal stability analysis of fusion proteins. **E** The Tm1 values showed the stability of the fusion proteins are strong. **F** The freeze–thaw stability analysis of fusion proteins by SEC-HPLC

ANGPTL3 at 0.352 nM (Fig. 2A, C). Both FD03-IL-1Ra and FD03 fusion proteins displayed similar high-binding affinities to the human or murine ANGPTL3 (Fig. 2B, C).

Previous studies have established that ANGPTL3 can inhibit the activity of LPL. Following this, the LPL activity assay was performed to assess the capacity of FD03-IL-1Ra and FD03 fusion protein on ANGPTL3 inhibition. These agents successfully counteracted the hindrance to LPL activity induced by hANGPTL3 (S17-K170). Notably, they showed IC50 values of 3.51 nM and 10.85 nM, respectively, outperforming evinacumab, which showed an IC50 value of 15.85 nM (Fig. 2D). Both FD03-IL-1Ra and FD03 fusion proteins exhibit high affinity to ANGPTL3 and possess robust biological activity.

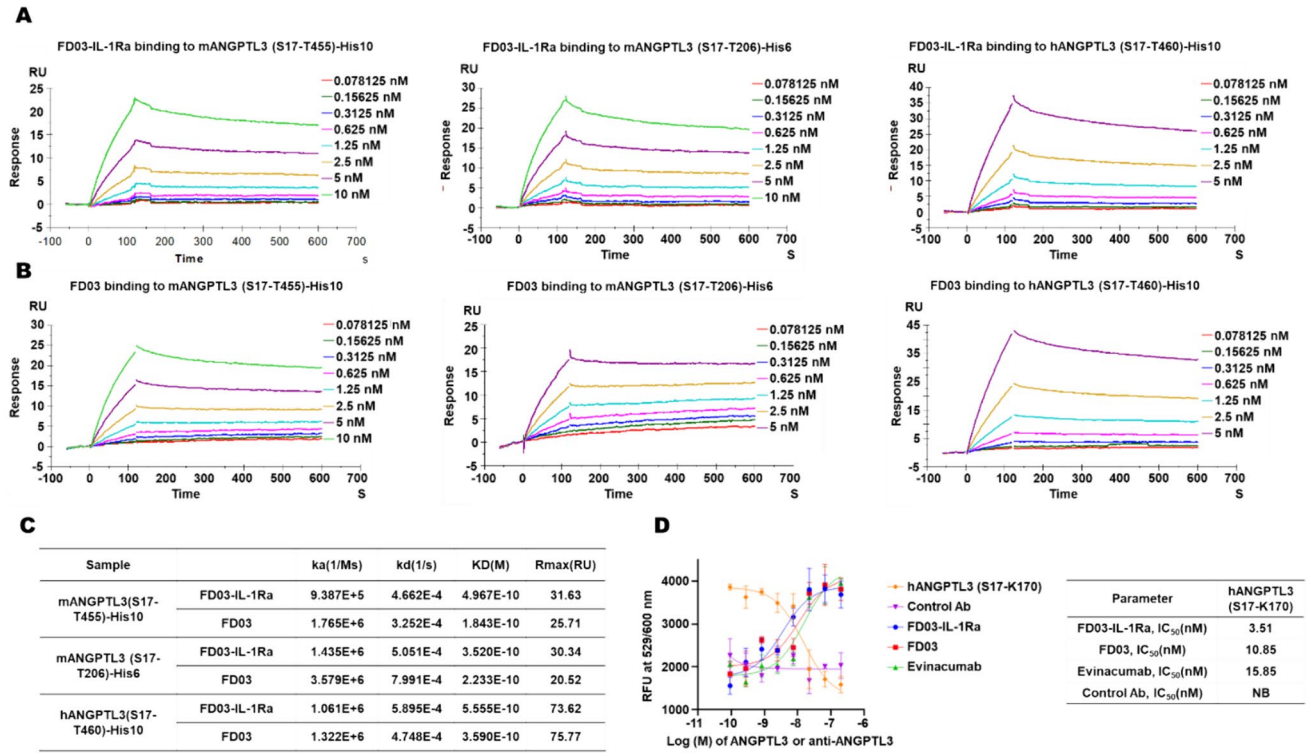

Sample		ka(1/Ms)	kd(1/s)	KD(M)	Rmax(RU)
mANGPTL3(S17-T455)-His10	FD03-IL-1Ra	9.387E+5	4.662E-4	4.967E-10	31.63
	FD03	1.765E+6	3.252E-4	1.843E-10	25.71
mANGPTL3 (S17-T206)-His6	FD03-IL-1Ra	1.435E+6	5.051E-4	3.520E-10	30.34
	FD03	3.579E+6	7.991E-4	2.233E-10	20.52
hANGPTL3(S17-T460)-His10	FD03-IL-1Ra	1.061E+6	5.895E-4	5.555E-10	73.62
	FD03	1.322E+6	4.748E-4	3.590E-10	75.77

Parameter	hANGPTL3 (S17-K170)
FD03-IL-1Ra, IC_{50}(nM)	3.51
FD03, IC_{50}(nM)	10.85
Evinacumab, IC_{50}(nM)	15.85
Control Ab, IC_{50}(nM)	NB

Fig. 2 Binding affinity and biological activity of FD03-IL-1Ra fusion protein against ANGPTL3. **A** The affinity of FD03-IL-1Ra binding to human full-length ANGPTL3, murine half-length ANGPTL3 and murine full-length ANGPTL3. **B** The affinity of FD03 binding to human full-length ANGPTL3, murine half-length ANGPTL3 and murine full-length ANGPTL3. **C** The affinity of FD03-IL-1Ra and FD03 binding to ANGPTL3 had no difference. **D** FD03 relieved the inhibitory effect of ANGPTL3 on LPL, which was detected by measuring fluorescence intensity of the lipase fluorescent substrate

FD03-IL-1Ra fusion protein could bind to IL-1R1 and inhibit IL-1β activity in vitro

To assess the binding affinity of the fusion protein with the IL-1 receptor (IL-1R), the affinity of FD03-IL-1Ra and IL-1Ra-Fc fusion proteins for both human and mouse IL-1R1 was investigated. FD03-IL-1Ra exhibited good affinity to hIL-1R1(18–332)-His6 at 0.9383 nM and mIL-1R1(20–338)-His6 at 5.137 nM, showing no significant difference from IL-1Ra-Fc (Fig. 3A–C). In cellular experiments, both FD03-IL-1Ra and IL-1Ra-Fc fusion proteins effectively inhibited IL-6 expression in A549 cells stimulated by IL-1β, with IC50 values of 0.1978 nM and 0.1984 nM, respectively, demonstrating no significant difference from the IC50 value of Anakinra. (Fig. 3D). Additionally, FD03-IL-1Ra and IL-1Ra-Fc fusion proteins could alleviate the growth inhibition of A375.S2 cells caused by IL-1β stimulation, with IC50 values of 0.2271 nM and 0.4131 nM. The IC50 of FD03-IL-1Ra was comparable to Anakinra (Fig. 3E). The fusion protein FD03-IL-1Ra demonstrated substantial binding affinity to both human and mouse IL-1R1, efficiently inhibited IL-6 expression in A549 cells, and alleviated growth inhibition in A375.S2 cells induced by IL-1β stimulation, suggesting its potential as a therapeutic agent for inflammatory conditions.

Serum lipids levels and lesion area of aorta were reduced in apoE$^{-/-}$ mice by FD03-IL-1Ra fusion protein treatment

To explore the potential therapeutic application of the FD03-IL-1Ra fusion protein in atherosclerosis, apoE$^{-/-}$ mice were subjected to an 8-week high-fat diet containing 1.25% cholesterol. Following this diet, the mice underwent continuous administration of the fusion protein for a duration of 5 weeks (Fig. 4A). As presented in Fig. 4B–D, TG, LDL-C and TC serum levels exhibited a significant and sustained decrease within the first week following the administration of atorvastatin, FD03 and FD03-IL-1Ra. Compared to the control group, no significant difference in the body weight of mice were observed (Fig. 4E). Continuous administration of atorvastatin, FD03 and FD03-IL-1Ra maintained the lipid-lowering effects consistently during the entire experimental cycle.

The white atherosclerotic plaques at the aortic arch showed a marked decrease in all treatment groups compared

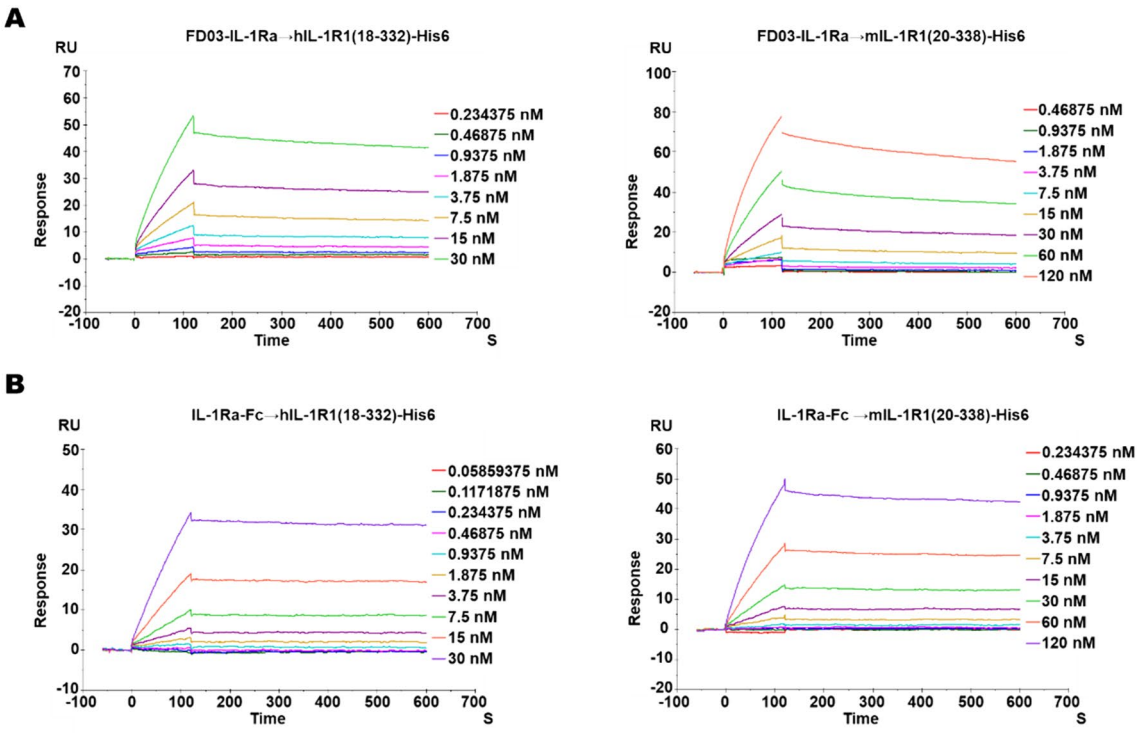

C

Sample		ka(1/Ms)	kd(1/s)	KD(M)	Rmax(RU)
hIL-1R1(18-332)-His6	FD03-IL-1Ra	2.670E+5	2.505E-4	9.383E-10	75.80
	IL-1Ra-Fc	8.143E+4	6.947E-5	8.543E-10	127.7
mIL-1R1(20-338)-His6	FD03-IL-1Ra	1.234E+6	6.341E-4	5.137E-9	98.63
	IL-1Ra-Fc	1.965E+5	2.492E-4	1.268E-9	62.86

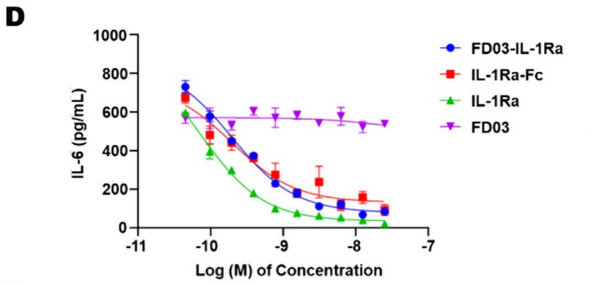

Parameter	IC_{50} (nM)
FD03-IL-1Ra	0.1978
IL-1Ra-Fc	0.1984
IL-1Ra	0.0728
FD03	NB

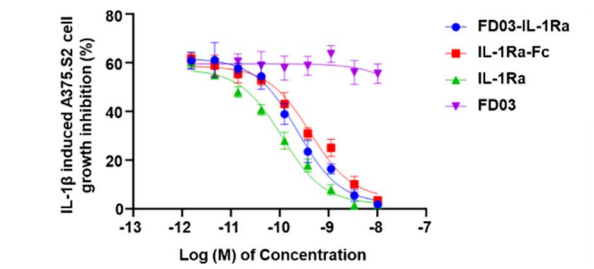

Parameter	IC_{50} (nM)
FD03-IL-1Ra	0.2271
IL-1Ra-Fc	0.4131
IL-1Ra	0.1098
FD03	NB

Fig. 3 FD03-IL-1Ra fusion protein could bind to IL-1R1 and inhibit IL-1β activity in vitro. **A** The affinity of FD03-IL-1Ra binding to hIL-1R1 (18–332)-His6 and mIL-1R1 (20–338)-His6. **B** The affinity of IL-1Ra-Fc binding to hIL-1R1 (18–332)-His6 and mIL-1R1 (20–338)-His6. **C** The affinity of FD03-IL-1Ra and IL-1Ra-Fc binding to IL-1R1 had no difference. **D** The fusion proteins FD03-IL-1Ra and IL-1Ra-Fc can inhibit IL-6 expression in A549 cells induced by IL-1β stimulation through binding to IL-1R. **E** FD03-IL-1Ra and IL-1Ra-Fc fusion proteins (n = 3) could eliminate the growth inhibition of A375.S2 cells caused by IL-1β stimulation

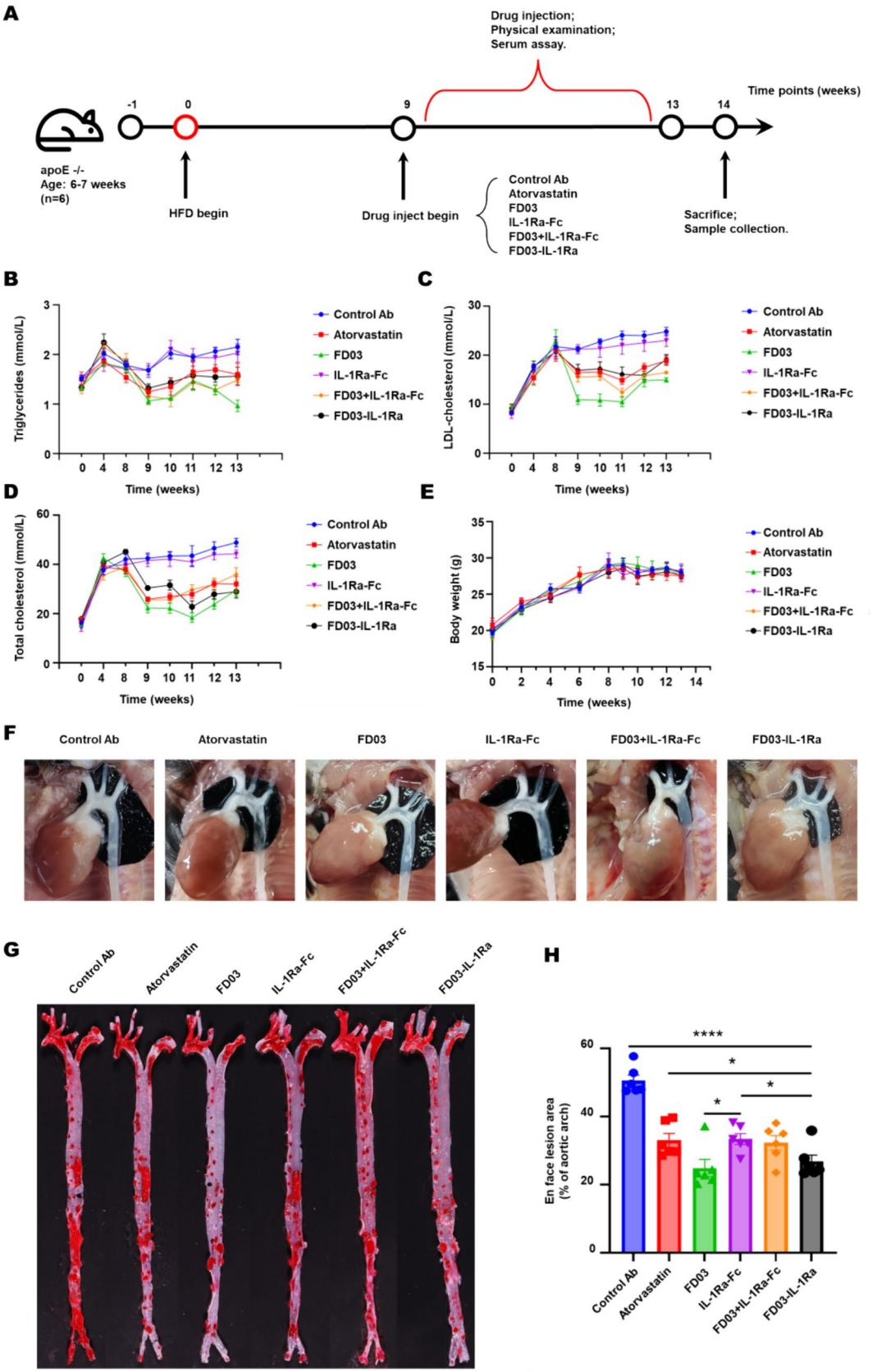
A
Drug injection;
Physical examination;
Serum assay.
Time points (weeks)
-1
0
9
13
14
apoE -/-
Age: 6-7 weeks
(n=6)
HFD begin
Drug inject begin
Control Ab
Atorvastatin
FD03
IL-1Ra-Fc
FD03+IL-1Ra-Fc
FD03-IL-1Ra
Sacrifice;
Sample collection.
B
Triglycerides (mmol/L)
Time (weeks)
C
LDL-cholesterol (mmol/L)
Time (weeks)
D
Total cholesterol (mmol/L)
Time (weeks)
E
Body weight (g)
Time (weeks)
F
Control Ab
Atorvastatin
FD03
IL-1Ra-Fc
FD03+IL-1Ra-Fc
FD03-IL-1Ra
G
Control Ab
Atorvastatin
FD03
IL-1Ra-Fc
FD03+IL-1Ra-Fc
FD03-IL-1Ra
H
En face lesion area
(% of aortic arch)
****
*
*
*

◂**Fig. 4** Serum lipids levels and lesion area of aorta were reduced in apoE$^{-/-}$ mice by FD03-IL-1Ra fusion protein treatment. **A** Experimental schematic. To assess the therapeutic effect of FD03-IL-1Ra on atherosclerotic mice following multiple dosing. Serum TG (**B**), LDL-C (**C**) and TC (**D**) levels on indicated groups were tested using assay kits. (n = 6). **E** The body weight of the mice. (F)Mouse aortic arch anatomies. **G**, **H** Mouse aortas were stained with Oil Red and the area of red staining was counted. $*P < 0.05; **P < 0.01; ***P < 0.001$

to the control group (Fig. 4F). The Oil Red staining analysis revealed a reduction in aortic plaque area across all treated groups (Fig. 4G, H). Remarkably, FD03-IL-1Ra and FD03 reduced the size of global plaque most effectively, surpassing the efficacy of IL-1Ra-Fc and atorvastatin. To evaluate the long-term safety, we conducted histological examinations on major organs after 5 weeks of administering FD03-IL-1Ra, IL-1Ra-Fc, or FD03. The results revealed no significant pathological damage (Supporting Data 1). In summary, the treatment of FD03-IL-1Ra fusion protein in atherosclerotic mice resulted in a significant reduction of the overall aortic plaque area. Additionally, a pronounced reduction was observed in the aortic sinus plaque area, surpassing the effects observed with FD03 and IL-1Ra-Fc when used alone. Importantly, FD03-IL-1Ra fusion protein also demonstrated the ability to enhance plaque stability, reducing necrotic lipid core area and mitigating plaque lipid infiltration.

FD03-IL-1Ra fusion protein reduced the area of atherosclerotic plaque and increased the stability of plaque in the aortic sinus

The size of aortic sinus plaques serves as an indicator of atherosclerotic disease progression. Aortic sinus sections underwent H&E staining to quantify the plaque area (Fig. 5A, D). In comparison to the control group, the FD03-IL-1Ra fusion protein significantly reduced the plaque area at the aortic sinus, demonstrating superior efficacy compared to FD03 and IL-1Ra-Fc alone. Furthermore, FD03-IL-1Ra fusion protein notably decreased lipid infiltration in aortic sinus plaques, showing a significant advantage over FD03 alone and the combinatory treatment. This observation was evidenced by ORO staining of aortic sinus sections (Fig. 5B, E).

Unstable plaques are prone to rupture, leading to acute coronary syndrome. Therefore, addressing changes in plaque stability is crucial in aspect of atherosclerosis treatment. Plaque stability is influenced by both collagen content and the size of the necrotic lipid core influence [28]. The collagen-rich regions were quantified as the blue portion in masson staining (Fig. 5C). Notably, an increase in collagen content was observed in all treatment groups, with the FD03-IL-1Ra fusion protein group exhibiting the highest collagen content in aortic sinus sections, significantly surpassing the FD03 treatment group (Fig. 5F). Simultaneously, the FD03-IL-1Ra fusion protein group displayed the smallest necrotic lipid core area in the aortic sinus, significantly lower than the FD03 group (Fig. 5G). The aforementioned studies demonstrated that FD03-IL-1Ra fusion protein exhibited advantages in reducing plaque lipid infiltration and enhancing plaque stability.

Oxidative stress and inflammatory responses in atherosclerotic plaques were suppressed by FD03-IL-1Ra fusion protein

Local inflammation plays a prominent role in atherosclerosis progression, making the assessment of local inflammation reduction crucial for evaluating therapeutic efficacy [29]. The accumulation of lipids and inflammatory cells instigate cytokine production, leading to the liberation of reactive oxygen species (ROS) that associated with atherosclerotic disease progression and acute coronary syndrome [28]. In the aortic sinus plaques of treated mice, ROS release was significantly diminished following treatment with FD03-IL-1Ra, as detected by the DCFH-DA fluorescent probe, exhibiting a marked contrast to the FD03 treatment group. Indicating that FD03-IL-1Ra enhances the anti-inflammatory effect, leading to a reduction in ROS release within the plaques. (Fig. 6A, C). Furthermore, the expression of 4-HNE, a byproduct of lipid peroxidation that induces chronic inflammatory responses and increases plaque instability, was remarkably reduced in response to the anti-inflammatory effect of the FD03-IL-1Ra fusion protein (Fig. 6B, D). This reduction suggests that the anti-inflammatory properties of FD03-IL-1Ra can inhibit the lipid peroxidation process within the aortic sinus plaques effectively.

The expression level of IL-1β, IL-6, and TNF-α was significantly reduced after five weeks treatment of FD03-IL-1Ra fusion protein (Fig. 6E–G). Notably, a more pronounced impact was observed in fusion protein on reducing serum IL-1β levels with FD03 or IL-1Ra-Fc treatment alone. Additionally, the FD03-IL-1Ra fusion protein markedly decreased serum IL-6 and TNF-α compared to FD03 treatment. These results collectively highlight the dual protective role of the fusion protein in treating atherosclerosis through simultaneous lipid-lowering and anti-inflammatory mechanisms.

Discussion

Current treatments for atherosclerosis primarily focus on lipid reduction; however, the condition continues to be associated with high mortality rates due to various complications [30, 31]. This study presents a pioneering therapeutic approach for atherosclerosis, which integrates

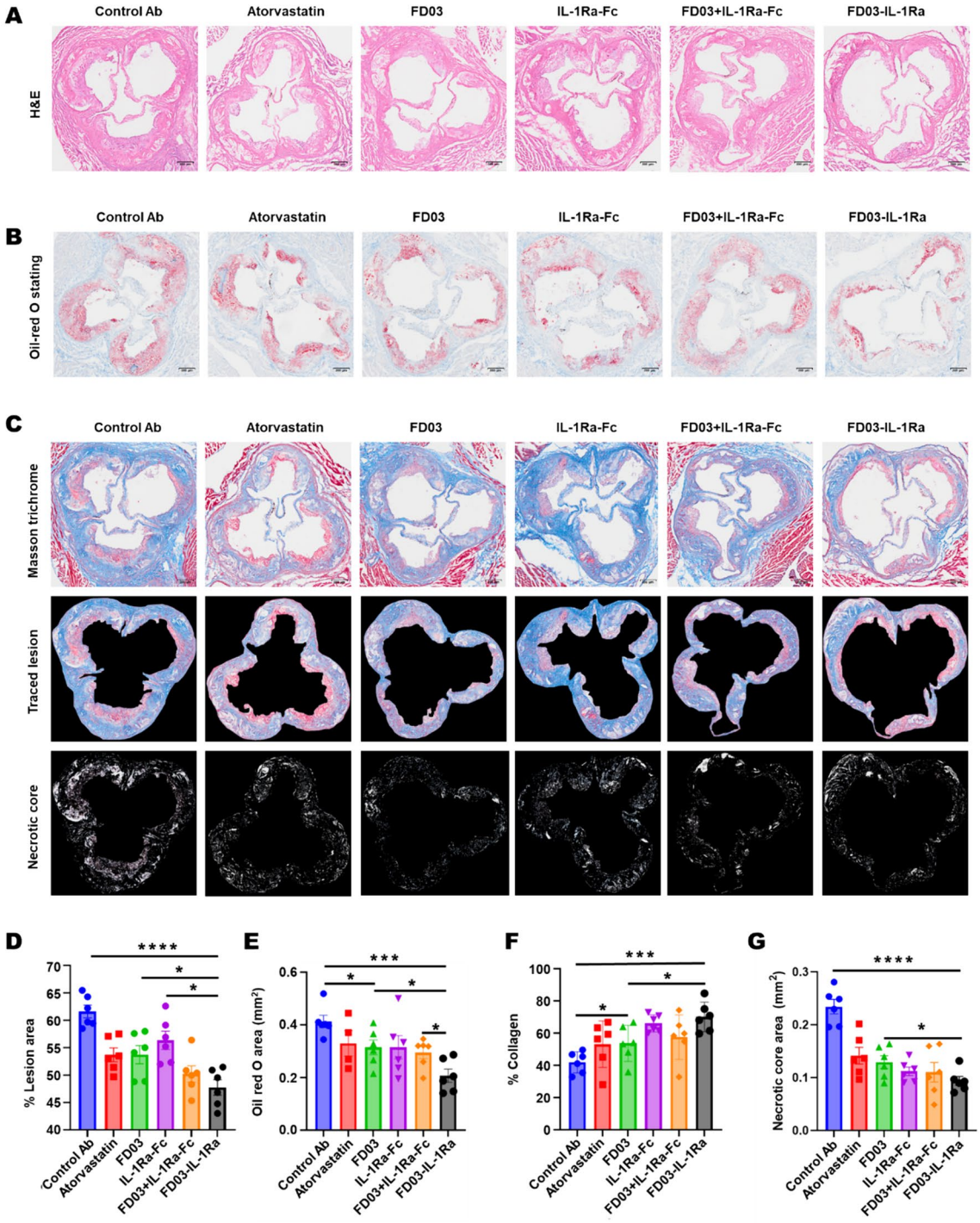

Fig. 5 FD03-IL-1Ra fusion protein reduced the atherosclerotic plaque area and increased the stability of plaque in aortic sinus. **A** Representative H&E, oil red O (**B**) and masson (**C**) stained images aortic sinus sections. Statistical analysis of lesion area (**D**, n = 6), Oil red O area (**E**, n = 6), percentage of collagen area (**F**, n = 6) and necrotic core area (**G**, n = 6). scale bar = 200 μm ∗ $P < 0.05$; ∗ ∗ $P < 0.01$; ∗ ∗ ∗ $P < 0.001$

the lipid-lowering and anti-inflammatory strategies. The efficacy of this treatment was confirmed through FD03-IL-1Ra, a newly developed fusion protein. Our findings indicate that this fusion protein reduces atherosclerotic lipid deposition by lowering low-density lipoprotein cholesterol in the blood, while simultaneously mitigating inflammatory responses and oxidative stress by inhibiting IL-1

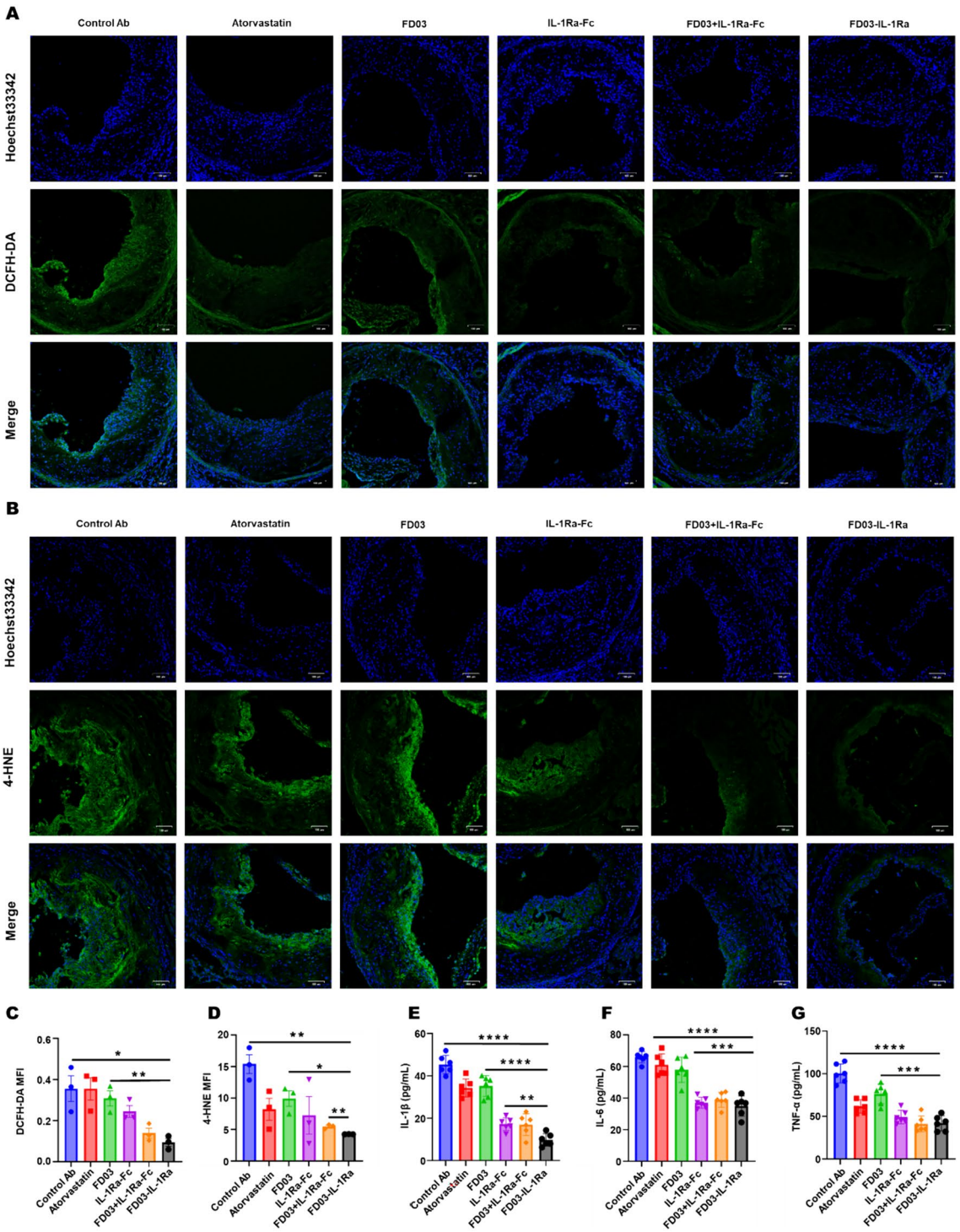

Fig. 6 Oxidative stress and inflammatory responses in atherosclerotic plaques were suppressed by FD03-IL-1Ra fusion protein. **A** DCFH-DA levels of aortic sinus were measured by immunofluorescence. **B** The levels of 4-HNE in the aortic sinus sections were measured by immunofluorescence. Statistical analysis of ROS (**C**, n = 3) and 4-HNE (**D**, n = 3). Levels of IL-1β (**E**, n = 6), IL-6 (**F**, n = 6) and TNF-α (**G**, n = 6) in serum of mice four days after the last administration. Scale bar = 100 μm. $*P < 0.05$; $**P < 0.01$; $***P < 0.001$

function. The invention of this agents effectively hinders the further advancement of atherosclerosis.

Numerous studies have substantiated the detrimental impact of low-density lipoprotein cholesterol on atherosclerosis [32, 33]. Inhibiting ANGPTL3 signaling has been shown to reactivate lipoprotein lipase, promoting the breakdown of lipoproteins [34]. Additionally, the use of ANGPTL3 nanobodies has demonstrated efficacy in reducing NAFLD model mice, leading to a significant improvement in hepatic fat accumulation and liver injury [12]. The therapeutic effect of atherosclerosis in mice can be achieved by reducing circulating LDL-C through the inhibition of PCSK9 and ANGPTL3 [35, 36]. In this study, we introduced the sequence of FD03, an ANGPTL3 nanobody, to construct a novel fusion protein. As anticipated, the FD03-IL-1Ra fusion protein effectively lowered circulating low-density lipoprotein cholesterol, mitigating the promoting effect of lipid deposition on atherosclerosis by inhibiting ANGPTL3 signaling.

It becomes evident that severe atherosclerotic plaques are often accompanied by increased lipid infiltration and a heightened inflammatory response [37, 38]. This is manifested by raised serum pro-inflammatory cytokines such as IL-1β and TNF-α, or a localized oxidative stress response within plaques, causing tissue damage and further fueling atherosclerosis progression [39]. Lowering lipid levels with atorvastatin or antagonizing ANGPTL3 can partially suppress inflammation [40]. However, the persistent inflammatory risk remains a critical factor in cardiovascular disease recurrence [41]. Therefore, simultaneous inhibition of inflammation alongside lipid-lowering therapy becomes imperative. FD03-IL-1Ra not only inhibited the upstream inflammatory factor IL-1β but also demonstrated a lipid-lowering effect comparable to atorvastatin. This dual action not only enhances the therapeutic efficacy against atherosclerosis but also mitigates the potential risk of cardiovascular diseases [42].

To address the inflammatory aspect, the other end of the fusion protein incorporates IL-1Ra, a human IL-1 antagonist. IL-1Ra competitively binds to IL-1R1, inhibiting IL-1 function. Research on IL-1 in atherosclerosis has revealed the unique effects of both IL-1α and IL-1β [43]. Senescent vascular smooth muscle cells (VSMC) can secrete multiple inflammatory cytokines in an IL-1α-dependent manner [44]. Clinical studies with canakinumab have demonstrated the therapeutic effect of IL-1β inhibition in atherosclerosis patients [45]. Furthermore, studies indicate that IL-1Ra not only hinders the development of atherosclerosis but also reduces the incidence of acute myocardial infarction and heart failure [46, 47]. We therefore chose IL-1Ra rather than IL-1β monoclonal antibodies to inhibit IL-1 function. In the results of the aortic Oil Red O staining (Fig. 4H), there was no significant difference between the FD03 group and the FD03-IL-1Ra group, suggesting that the introduction of IL-1Ra did not reduce the plaque area in the aorta. However, this does not imply that the introduction of IL-1Ra is ineffective. The assessment of atherosclerosis progression involves not only measuring plaque area but also evaluating plaque stability and the extent of lipid and inflammatory infiltration. Data from the aortic sinus sections indicate that the introduction of anti-inflammatory cytokines reduced lipid infiltration, increased plaque stability, and decreased the risk of acute coronary syndrome. Furthermore, it lowered the overall inflammatory levels in the serum of the mice.

In this study, we focused on the free form of ANGPTL3 and inhibited its antagonistic activity on LPL. ANGPTL3 can influence the progression of atherosclerosis through both lipid and non-lipid mechanisms [48]. Structurally, ANGPTL3 is composed of a coiled-coil domain (CCD) and a fibrinogen-like domain (FLD). FD03 is an antibody that targets the CCD, but its potential effects on the function of the FLD in vivo remain to be further investigated. The FLD affects arterial wall thickness and macrophage activity and can lead to angiogenesis, foam cell formation, inflammation, and apoptosis by binding to integrin αVβ3. This interaction has been demonstrated in models of kidney injury and human retinal microvascular endothelial cells [49, 50]. Integrin αVβ3 is closely associated with the formation of atherosclerotic plaques. Therefore, exploring the role of ANGPTL3 and αVβ3 in atherosclerosis could deepen our understanding of the disease. Studies have shown that αVβ3 can promote monocyte migration across endothelial cells and enhance adhesion between platelets and the vascular endothelium, thereby upregulating monocyte chemotactic protein-1 (MCP-1) and intercellular adhesion molecule-1 (ICAM-1) expression through an IL-1-dependent mechanism and exacerbating atherosclerosis [51]. The addition of IL-1Ra can reduce the expression of MCP-1 and ICAM-1 via the nuclear factor-κB (NF-κB) signaling pathway and decrease adhesion between platelets and the vascular endothelium [52]. This provides a new explanation for the therapeutic effects of the FD03-IL-1Ra fusion protein.

In terms of protein design, FD03-IL-1Ra strategically combines two proteins with smaller molecular weights—nanobodies and cytokines. This approach aims to mitigate potential immunogenicity issues associated with larger protein molecular weights. Simultaneously, a mutated human IgG1 Fc was chosen to link the ANGPTL3 nanobody and IL-1Ra, extending the half-life of the fusion protein. SPR and biological experiments in vitro confirmed that this protein design strategy did not compromise the functionality of both ends of the fusion protein. Moreover, this design exhibits favorable solubility and stability, indicating its potential for further development.

Based on the findings of this study, FD03-IL-1Ra, functioning as a fusion protein capable of inhibiting both

ANGPTL3 and IL-1, demonstrates substantial therapeutic effects by decreasing low-density lipoprotein cholesterol and alleviating local inflammatory responses within plaques in mouse models. It holds promise as a potential candidate for treating atherosclerosis or other conditions characterized by a combination of inflammation and lipid deposition, such as nonalcoholic steatohepatitis (NASH). Nevertheless, further investigations are warranted to delve into the intricate mechanisms linking lipid metabolism and IL-1 in atherosclerosis.

Supplementary Information The online version contains supplementary material available at https://doi.org/10.1007/s00011-024-01941-1.

Acknowledgements This work was supported by grants from National Key Research and Development Program of China (2023YFC3404000) and the National Natural Science Foundation of China (82371781 and 82073752).

Author contributions Hanqi Wang conducted the experiments and drafted the article. Xiaozhi Hu and Yuting Zhang were involved in revising the article and designing experiments. An Zhu and Jiajun Fan played key roles in designing and conducting animal experiments, as well as revising the manuscript. Zhengyu Wu, Xuebin Wang, and Wei Hu provided valuable input for the experimental design and offered support in terms of equipment and funding. Dianwen Ju contributed to the design of the experiment, revised the manuscript, and provided substantial support in terms of experimental equipment and funding.

Data availability No datasets were generated or analysed during the current study.

Declarations

Conflict of interest The authors declare no conflicts of interest.

References

1. Mendis S, Davis S, Norrving B. Organizational update: the world health organization global status report on noncommunicable diseases 2014; one more landmark step in the combat against stroke and vascular disease. Stroke. 2015;46(5):e121–2.
2. Chapman MJ. Therapeutic elevation of HDL-cholesterol to prevent atherosclerosis and coronary heart disease. Pharmacol Ther. 2006;111(3):893–908.
3. Seidah NG, Garçon D. Expanding biology of PCSK9: roles in atherosclerosis and beyond. Curr Atheroscler Rep. 2022;24(10):821–30.
4. Almeida SO, Budoff M. Effect of statins on atherosclerotic plaque. Trends Cardiovasc Med. 2019;29(8):451–5.
5. Silverman MG, Ference BA, Im K, et al. Association between lowering LDL-C and cardiovascular risk reduction among different therapeutic interventions: a systematic review and meta-analysis. JAMA. 2016;316(12):1289–97.
6. Abdul-Rahman T, Bukhari SMA, Herrera EC, et al. Lipid lowering therapy: an era beyond statins. Curr Probl Cardiol. 2022;47(12): 101342.
7. Thompson PD, Panza G, Zaleski A, Taylor B. Statin-associated side effects. J Am Coll Cardiol. 2016;67(20):2395–410.
8. Quagliarini F, Wang Y, Kozlitina J, et al. Atypical angiopoietin-like protein that regulates ANGPTL3. Proc Natl Acad Sci U S A. 2012;109(48):19751–6.
9. Kersten S. Physiological regulation of lipoprotein lipase. Biochim Biophys Acta. 2014;1841(7):919–33.
10. Stitziel NO, Khera AV, Wang X, et al. ANGPTL3 deficiency and protection against coronary artery disease. J Am Coll Cardiol. 2017;69(16):2054–63.
11. Dewey FE, Gusarova V, Dunbar RL, et al. Genetic and pharmacologic inactivation of ANGPTL3 and cardiovascular disease. N Engl J Med. 2017;377(3):211–21.
12. Hu X, Fan J, Ma Q, et al. A novel nanobody-heavy chain antibody against Angiopoietin-like protein 3 reduces plasma lipids and relieves nonalcoholic fatty liver disease. J Nanobiotechnol. 2022;20(1):237.
13. Hada Y, Uchida HA, Mukai T, et al. Inhibition of interleukin-6 signaling attenuates aortitis, left ventricular hypertrophy and arthritis in interleukin-1 receptor antagonist deficient mice. Clin Sci (Lond). 2020;134(20):2771–87.
14. Cuchel M, Raal FJ, Hegele RA, et al. 2023 Update on European Atherosclerosis Society Consensus Statement on Homozygous Familial Hypercholesterolaemia: new treatments and clinical guidance. Eur Heart J. 2023;44(25):2277–91.
15. Mai W, Liao Y. Targeting IL-1β in the Treatment of Atherosclerosis. Front Immunol. 2020;11: 589654.
16. Dinarello CA. Biologic basis for interleukin-1 in disease. Blood. 1996;87(6):2095–147.
17. Pedersen BK. Anti-inflammatory effects of exercise: role in diabetes and cardiovascular disease. Eur J Clin Invest. 2017;47(8):600–11.
18. Buckley LF, Abbate A. Interleukin-1 blockade in cardiovascular diseases: a clinical update. Eur Heart J. 2018;39(22):2063–9.
19. Orecchioni M, Kobiyama K, Winkels H, et al. Olfactory receptor 2 in vascular macrophages drives atherosclerosis by NLRP3-dependent IL-1 production. Science. 2022;375(6577):214–21.
20. Chi H, Messas E, Levine RA, Graves DT, Amar S. Interleukin-1 receptor signaling mediates atherosclerosis associated with bacterial exposure and/or a high-fat diet in a murine apolipoprotein E heterozygote model: pharmacotherapeutic implications. Circulation. 2004;110(12):1678–85.
21. Isoda K, Sawada S, Ishigami N, et al. Lack of interleukin-1 receptor antagonist modulates plaque composition in apolipoprotein E-deficient mice. Arterioscler Thromb Vasc Biol. 2004;24(6):1068–73.
22. Huang Y, Ma K, Qin R, Fang Y, Zhou J, Dai X. Pristane attenuates atherosclerosis in Apoe(-/-) mice via IL-4-secreting regulatory plasma cell-mediated M2 macrophage polarization. Biomed Pharmacother. 2022;155: 113750.
23. Kirii H, Niwa T, Yamada Y, et al. Lack of interleukin-1beta decreases the severity of atherosclerosis in ApoE-deficient mice. Arterioscler Thromb Vasc Biol. 2003;23(4):656–60.
24. Van Tassell BW, Trankle CR, Canada JM, et al. IL-1 blockade in patients with heart failure with preserved ejection fraction. Circ Heart Fail. 2018;11(8): e005036.
25. Van Tassell BW, Canada J, Carbone S, et al. Interleukin-1 blockade in recently decompensated systolic heart failure: results From REDHART (Recently Decompensated Heart Failure Anakinra Response Trial). Circ Heart Fail. 2017;10(11): e004373.
26. Wu C, Mao J, Wang X, et al. Advances in treatment strategies based on scavenging reactive oxygen species of nanoparticles for atherosclerosis. J Nanobiotechnology. 2023;21(1):271.
27. Mali VR, Palaniyandi SS. Regulation and therapeutic strategies of 4-hydroxy-2-nonenal metabolism in heart disease. Free Radic Res. 2014;48(3):251–63.
28. Hu R, Dai C, Dong C, et al. Living macrophage-delivered tetrapod PdH nanoenzyme for targeted atherosclerosis management by ROS scavenging, hydrogen anti-inflammation, and autophagy activation. ACS Nano. 2022;16(10):15959–76.

29. Gimbrone MA Jr, García-Cardeña G. Endothelial cell dysfunction and the pathobiology of atherosclerosis. Circ Res. 2016;118(4):620–36.
30. Libby P. The changing landscape of atherosclerosis. Nature. 2021;592(7855):524–33.
31. Zhang Y, Zhu Z, Cao Y, et al. Rnd3 suppresses endothelial cell pyroptosis in atherosclerosis through regulation of ubiquitination of TRAF6. Clin Transl Med. 2023;13(9): e1406.
32. Hartley A, Haskard D, Khamis R. Oxidized LDL and anti-oxidized LDL antibodies in atherosclerosis—novel insights and future directions in diagnosis and therapy<sup/>. Trends Cardiovasc Med. 2019;29(1):22–6.
33. Lydic TA, Goo YH. Lipidomics unveils the complexity of the lipidome in metabolic diseases. Clin Transl Med. 2018;7(1):4.
34. Mohamed F, Mansfield BS, Raal FJ. ANGPTL3 as a drug target in hyperlipidemia and atherosclerosis. Curr Atheroscler Rep. 2022;24(12):959–67.
35. Ding Z, Pothineni NVK, Goel A, Lüscher TF, Mehta JL. PCSK9 and inflammation: role of shear stress, pro-inflammatory cytokines, and LOX-1. Cardiovasc Res. 2020;116(5):908–15.
36. Sabatine MS. PCSK9 inhibitors: clinical evidence and implementation. Nat Rev Cardiol. 2019;16(3):155–65.
37. Kong P, Cui ZY, Huang XF, Zhang DD, Guo RJ, Han M. Inflammation and atherosclerosis: signaling pathways and therapeutic intervention. Signal Transduct Target Ther. 2022;7(1):131.
38. Li Q, Yu L, Gao A, et al. METTL3 (Methyltransferase Like 3)-dependent N6-methyladenosine modification on Braf mRNA promotes macrophage inflammatory response and atherosclerosis in mice. Arterioscler Thromb Vasc Biol. 2023;43(5):755–73.
39. Ridker PM, Lüscher TF. Anti-inflammatory therapies for cardiovascular disease. Eur Heart J. 2014;35(27):1782–91.
40. Ridker PM, Bhatt DL, Pradhan AD, Glynn RJ, MacFadyen JG, Nissen SE. Inflammation and cholesterol as predictors of cardiovascular events among patients receiving statin therapy: a collaborative analysis of three randomised trials. Lancet. 2023;401(10384):1293–301.
41. Ridker PM. Targeting residual inflammatory risk: the next frontier for atherosclerosis treatment and prevention. Vascul Pharmacol. 2023;153: 107238.
42. Ridker PM. From C-Reactive Protein to Interleukin-6 to Interleukin-1: Moving Upstream To Identify Novel Targets for Atheroprotection. Circ Res. 2016;118(1):145–56.
43. Vromman A, Ruvkun V, Shvartz E, et al. Stage-dependent differential effects of interleukin-1 isoforms on experimental atherosclerosis. Eur Heart J. 2019;40(30):2482–91.
44. Yu H, Clarke MC, Figg N, Littlewood TD, Bennett MR. Smooth muscle cell apoptosis promotes vessel remodeling and repair via activation of cell migration, proliferation, and collagen synthesis. Arterioscler Thromb Vasc Biol. 2011;31(11):2402–9.
45. Ridker PM, MacFadyen JG, Thuren T, Everett BM, Libby P, Glynn RJ. Effect of interleukin-1β inhibition with canakinumab on incident lung cancer in patients with atherosclerosis: exploratory results from a randomised, double-blind, placebo-controlled trial. Lancet. 2017;390(10105):1833–42.
46. Busch K, Kny M, Huang N, et al. Inhibition of the NLRP3/IL-1β axis protects against sepsis-induced cardiomyopathy. J Cachexia Sarcopenia Muscle. 2021;12(6):1653–68.
47. Abbate A, Toldo S, Marchetti C, Kron J, Van Tassell BW, Dinarello CA. Interleukin-1 and the inflammasome as therapeutic targets in cardiovascular disease. Circ Res. 2020;126(9):1260–80.
48. Lupo MG, Ferri N. Angiopoietin-like 3 (ANGPTL3) and atherosclerosis: lipid and non-lipid related effects. J Cardiovasc Dev Dis. 2018;5(3):39.
49. Wang N, Zou C, Zhao S, Wang Y, Han C, Zheng Z. Fenofibrate exerts protective effects in diabetic retinopathy via inhibition of the ANGPTL3 pathway. Invest Ophthalmol Vis Sci. 2018;59(10):4210–7.
50. Ma Q, Hu X, Liu F, et al. A novel fusion protein consisting of anti-ANGPTL3 antibody and interleukin-22 ameliorates diabetic nephropathy in mice. Front Immunol. 2022;13:1011442.
51. Gawaz M, Brand K, Dickfeld T, et al. Platelets induce alterations of chemotactic and adhesive properties of endothelial cells mediated through an interleukin-1-dependent mechanism. Implications for atherogenesis. Atherosclerosis. 2000;148(1):75–85.
52. Zhang Y, Zhang ZT, Wan SY, et al. ANGPTL3 negatively regulates IL-1β-induced NF-κB activation by inhibiting the IL1R1-associated signaling complex assembly. J Mol Cell Biol. 2024;15(8):mjad053.

Authors and Affiliations

Hanqi Wang[1,2] · Xiaozhi Hu[2] · Yuting Zhang[2] · An Zhu[2] · Jiajun Fan[2] · Zhengyu Wu[3] · Xuebin Wang[4] · Wei Hu[1] · Dianwen Ju[1,2]

✉ Xuebin Wang
binxuewang@sjtu.edu.cn

✉ Wei Hu
hu_wei@fudan.edu.cn

✉ Dianwen Ju
dianwenju@fudan.edu.cn

[1] Department of Cardiology, Minhang Hospital, Fudan University, No. 170 Zisong Road, Minhang District, Shanghai, China

[2] Department of Biological Medicines & Shanghai Engineering Research Center of Immunotherapeutics, Fudan University School of Pharmacy, No. 826 Zhangheng Road, Pudong New District, Shanghai, China

[3] TAU Cambridge Ltd, The Bradfield Centre UNIT 184, Cambridge Science Park, Cambridge CB4 0GA, UK

[4] Department of Pharmacy, Shanghai Children's Hospital, School of Medicine, Shanghai Jiao Tong University, 355 Luding Road, Putuo District, Shanghai, China